

Oxime Ethers of (*E*)-11-Isonitrosostrychnine as Highly Potent Glycine Receptor Antagonists

Amal M. Y. Mohsen,[†] Yasmine M. Mandour,[†] Edita Sarukhanyan,[‡] Ulrike Breitinge,[†] Carmen Villmann,[‡] Maha M. Banoub,[†] Hans-Georg Breitinge,[†] Thomas Dandekar,[‡] Ulrike Holzgrabe,[§] Christoph Sotriffer,[§] Anders A. Jensen,^{||} and Darius P. Zlotos^{*,†}

[†]Faculty of Pharmacy and Biotechnology, The German University in Cairo, New Cairo City, 11835 Cairo, Egypt

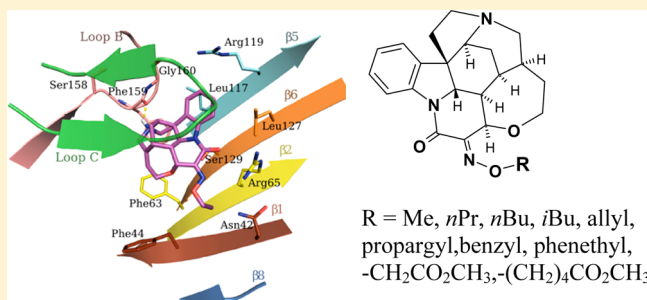
[‡]Biocenter, Department of Bioinformatics and [§]Institute of Pharmacy and Food Chemistry, University of Würzburg, 97074 Würzburg, Germany

[‡]Institute of Clinical Neurobiology, University of Würzburg, 97078 Würzburg, Germany

^{||}Department of Drug Design and Pharmacology, Faculty of Health and Medical Sciences, University of Copenhagen, DK-2100 Copenhagen, Denmark

Supporting Information

ABSTRACT: A series of (*E*)-11-isonitrosostrychnine oxime ethers, 2-aminostrychnine, (strychnine-2-yl)propionamide, 18-oxostrychnine, and *N*-propylstrychnine bromide were synthesized and evaluated pharmacologically at human $\alpha 1$ and $\alpha 1\beta$ glycine receptors in a functional fluorescence-based and a whole-cell patch-clamp assay and in [³H]strychnine binding studies. 2-Aminostrychnine and the methyl, allyl, and propargyl oxime ethers were the most potent $\alpha 1$ and $\alpha 1\beta$ antagonists in the series, displaying IC₅₀ values similar to those of strychnine at the two receptors. Docking experiments to the strychnine binding site of the crystal structure of the $\alpha 3$ glycine receptor indicated the same orientation of the strychnine core for all analogues. For the most potent oxime ethers, the ether substituent was accommodated in a lipophilic receptor binding pocket. The findings identify the oxime hydroxy group as a suitable attachment point for linking two strychnine pharmacophores by a polymethylene spacer and are, therefore, important for the design of bivalent ligands targeting glycine receptors.



Strychnine, the major alkaloid from the plant *Strychnos nuxvomica*, exhibits pharmacological activity at several neurotransmitter receptors, including a number of ligand-gated ion channels, such as muscle-type and neuronal nicotinic acetylcholine receptors and glycine receptors (GlyRs). The major pharmacological action of strychnine is a strong antagonistic activity at the latter receptors, which are often referred to as strychnine-sensitive GlyRs.^{1–3} The GlyRs are anion-selective channels that mediate inhibitory synaptic transmission in the spinal cord and brainstem, and they are believed to play crucial roles in motor coordination and pain signal transmission.^{4,5} Disruption of the normal GlyR function caused by heritable mutations is associated with neuromotor disorders such as hyperekplexia or some forms of spasticity.^{5–8} The GlyRs are pentameric subunit complexes belonging to the superfamily of Cys-loop receptors and exist either as homomers composed of α subunits or heteromers that contain both α and β subunits.⁹ While four α -subunit isoforms are known ($\alpha 1$ – $\alpha 4$), only one β subunit has been identified. The precise distribution of different subunits is specific to different parts of the central nervous system.^{10,11}

For a long time, understanding of the molecular mechanisms of GlyR function has been hampered by a lack of high-resolution structures of the receptors, and only recently have homology models based on structures of other Cys-loop receptors become available.¹² Recently, however, electro-cryo-microscopy structures of the zebra fish $\alpha 1$ GlyR in complex with strychnine and glycine¹³ and a crystal structure of human $\alpha 3$ GlyR in complex with strychnine¹⁴ have been published, providing a detailed insight into the molecular recognition of agonists and antagonists and mechanisms of GlyR activation and inactivation.

The natural product strychnine has been optimized for strong interactions with biological macromolecules through evolutionary selection. Indeed, it displays nanomolar binding affinity and inhibitory potency at recombinant and native GlyRs in binding studies and functional assays.^{2,3,15} In previous structure–activity relationship (SAR) studies any structural change to strychnine, including N-quaternization, C-2-nitration, lactam reduction, hydrogenation, oxidation, or relocation of the

Received: May 24, 2016

C-21–C-22 double bond, and opening of the tetrahydrooxepine ring, has been reported to decrease the antagonist activity at GlyRs.^{16–18} The only structure modification not to impair the activity of the parent compound is the introduction of an *E*-configured hydroxyimino group at C-11 to give (*E*)-11-isonitrosostrychnine (**1**). Similar to strychnine, none of these analogues exhibited selectivity between homomeric $\alpha 1$ and heteromeric $\alpha 1\beta$ receptors.

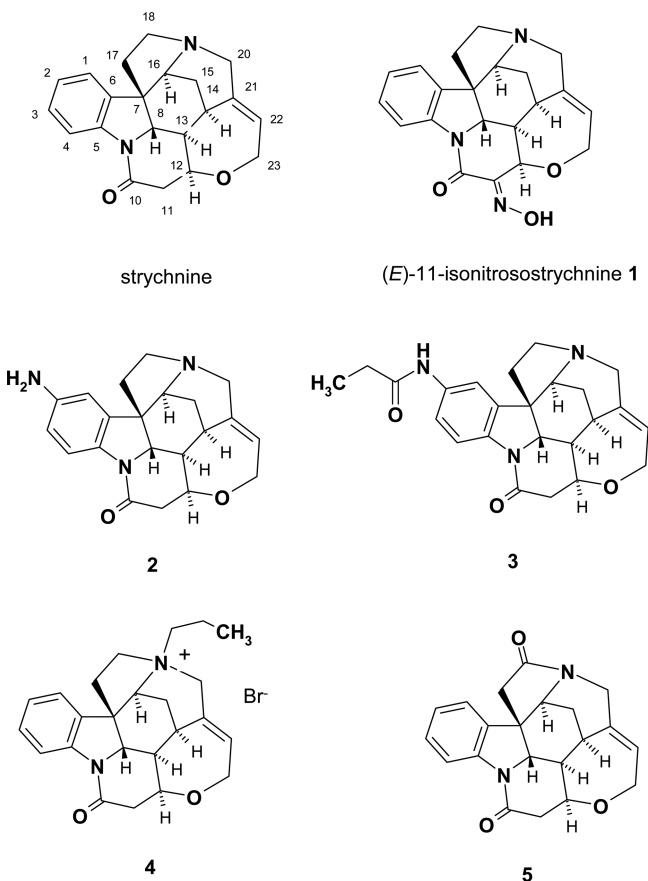
Recently, our groups have become interested in a bivalent ligand approach for targeting GlyRs. Bivalent ligands are compounds that comprise two chemical groups (pharmacophores) linked to each other by a spacer of a specific length and composition and are potentially capable of simultaneous binding to two distinct binding sites. On the basis of its high potency and a good understanding of SAR, strychnine represents an excellent pharmacophore for bivalent ligands targeting GlyRs. Since the C-11 (*E*)-hydroxyimino functional group of compound **1** secured its high antagonistic potency, an oxime ether linkage appears to be suitable for the attachment of the spacer. In order to examine the impact of an alkyl substituent attached to the hydroxy group of **1** on the antagonist potency, an extensive series of strychnine oxime ethers have been synthesized and evaluated pharmacologically in the current work. Additionally, to explore the C-2 amide group of strychnine as another potential linker for strychnine-based bivalent ligands, (strychnine-2-yl)propionamide (**3**) was synthesized and pharmacologically evaluated. Finally, to extend the SAR of strychnine at GlyRs, 2-aminostrychnine (**2**), *N*-propylstrychnine bromide (**4**), and 18-oxostrychnine (**5**) were included in the study. The SAR findings are discussed based on docking experiments using the high-resolution crystal structure of $\alpha 3$ GlyR with strychnine occupying its orthosteric binding site.¹⁴

RESULTS AND DISCUSSION

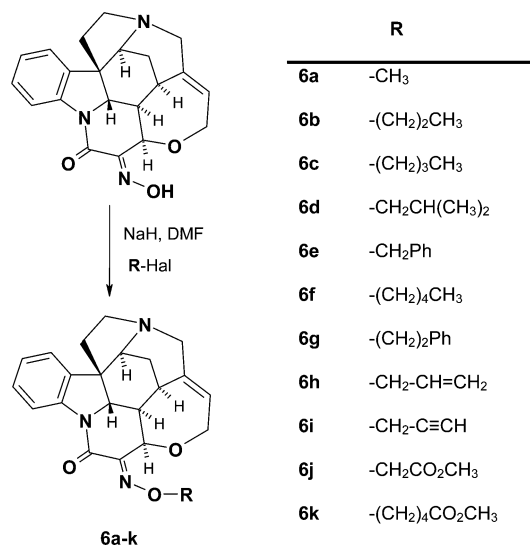
The structures of the strychnine analogues studied in this work are shown in Chart 1 and Scheme 1. (*E*)-11-Isonitrosostrychnine (**1**) was obtained by nitrosation of strychnine using *tert*-butyl nitrite/*tert*-BuOK as previously reported.¹⁹ 2-Aminostrychnine (**2**) was synthesized in a two-step approach by nitration of strychnine and subsequent reduction of the nitro group using SnCl₂.²⁰ 2-Propionamidostychnine (**3**) was obtained by acylation of 2-aminostrychnine using propionic acid anhydride. *N*-Propylstrychnine bromide (**4**) was prepared by quaternization of strychnine using *n*-propyl bromide as previously reported.²¹ 18-Oxostrychnine (**5**) was synthesized from strychnine *N*-oxide using K₂Cr₂O₇ according to a modified procedure by Rosenmund and co-workers.²² The oxime ethers **6a–k** were synthesized by O-alkylation of **1** using NaH as a base and an appropriate alkylating agent.

The functional properties of compounds **2–5** and **6a–k** and the reference ligands strychnine and (*E*)-11-isonitrosostrychnine (**1**) were characterized at the human $\alpha 1$ and $\alpha 1\beta$ receptor subtypes in the fluorescence-based FLIPR membrane potential blue (FMP) assay. Here, the receptors were transiently expressed in tsA201 cells, and the abilities of the compounds to inhibit the response induced by glycine EC₅₀ (EC₄₀–EC₆₀) in the cells were determined.²³ The expression of homogeneous populations of $\alpha 1$ and $\alpha 1\beta$ receptors in the cells was verified on a routine basis using picrotoxin, which as previously reported displays ~100-fold higher antagonist potency at $\alpha 1$ than at $\alpha 1\beta$ in this assay.²⁴ The IC₅₀ values determined for the compounds are given in Table 1.

Chart 1



Scheme 1



Previous SAR studies have identified the lactam carbonyl group, the tertiary amino group, and the C-21–C-22 double bond in strychnine as essential structural elements required for its strong antagonistic activity at homo- and heteromeric GlyRs.^{16–18} These findings are in agreement with the recently published experimental structures of strychnine bound to the homomeric $\alpha 1$ and $\alpha 3$ GlyRs.^{13,14} The residues critical for strychnine binding are identical in the two receptors, resulting in the same antagonist binding mode. The orthosteric binding

Table 1. Pharmacological Characterization of the Compounds at $\alpha 1$ and $\alpha 1\beta$ GlyRs

	IC ₅₀ [μ M] FMP assay ^a		IC ₅₀ [μ M] patch-clamp assay ^b	
	$\alpha 1$	$\alpha 1\beta$	$\alpha 1$	$\alpha 1\beta$
strychnine	0.093 [7.03 \pm 0.09]	0.18 [6.74 \pm 0.06]	0.051 \pm 0.005	0.058 \pm 0.003
1	0.097 [7.01 \pm 0.03]	0.21 [6.67 \pm 0.10]	0.082 \pm 0.010	0.080 \pm 0.008
2	0.077 [7.11 \pm 0.08]	0.27 [6.56 \pm 0.05]	0.076 \pm 0.009	0.097 \pm 0.011
3	0.54 [6.27 \pm 0.05]	0.94 [6.03 \pm 0.08]	0.201 \pm 0.019	0.311 \pm 0.039
4	10 [4.98 \pm 0.07]	13 [4.87 \pm 0.05]	4.59 \pm 0.41	6.53 \pm 0.59
5	6.9 [5.16 \pm 0.04]	9.8 [5.00 \pm 0.16]		
6a	0.10 [6.98 \pm 0.09]	0.21 [6.67 \pm 0.05]	0.075 \pm 0.008	0.056 \pm 0.011
6b	0.11 [6.94 \pm 0.09]	0.35 [6.45 \pm 0.08]	0.109 \pm 0.009	0.116 \pm 0.018
6c	0.37 [6.42 \pm 0.05]	0.88 [6.06 \pm 0.03]		
6d	0.26 [6.58 \pm 0.07]	1.10 [5.95 \pm 0.06]		
6e	0.17 [6.78 \pm 0.13]	0.31 [6.51 \pm 0.06]		
6f	0.25 [6.61 \pm 0.10]	0.71 [6.15 \pm 0.08]		
6g	0.69 [6.15 \pm 0.07]	0.78 [6.11 \pm 0.08]		
6h	0.095 [7.02 \pm 0.03]	0.15 [6.80 \pm 0.04]	0.049 \pm 0.004	0.046 \pm 0.0049
6i	0.052 [7.29 \pm 0.10]	0.24 [6.62 \pm 0.13]	0.059 \pm 0.008	0.043 \pm 0.007
6j	0.22 [6.65 \pm 0.09]	0.67 [6.18 \pm 0.06]		
6k	0.72 [6.15 \pm 0.04]	1.50 [5.83 \pm 0.08]		

^aFunctional properties of the compounds at the human $\alpha 1$ and $\alpha 1\beta$ GlyRs transiently expressed in tsA201 cells in the FLIPR membrane potential blue (FMP) assay. EC₅₀ (EC₄₀–EC₆₀) concentrations of glycine were used as agonist at the two receptors (EC₅₀ = 42 μ M at $\alpha 1$, EC₅₀ = 23 μ M at $\alpha 1\beta$). The IC₅₀ values for the analogues represent the antagonistic potency and are given in μ M with pIC₅₀ \pm SEM in brackets. Data are given as the means based on $n = 3, 4$. ^bDirect inhibition of glycine-mediated currents was measured using whole-cell patch clamp recordings from HEK293 cells transiently transfected with GlyR $\alpha 1$ or $\alpha 1\beta$ cDNA. After determination of EC₅₀, strychnine derivatives in varying concentrations were perfused over GlyR-expressing cells and inhibition curves constructed from whole-cell current amplitudes measured in the presence and absence of inhibitor at EC₅₀ concentrations of glycine. IC₅₀ values were determined from inhibition curves constructed from a nonlinear fit to dose–response data using 4–7 cells per inhibitor. Data are given as means \pm SEM.

site of the homomeric $\alpha 3$ receptor with docked strychnine is shown in Figure 2A. The most important binding interactions

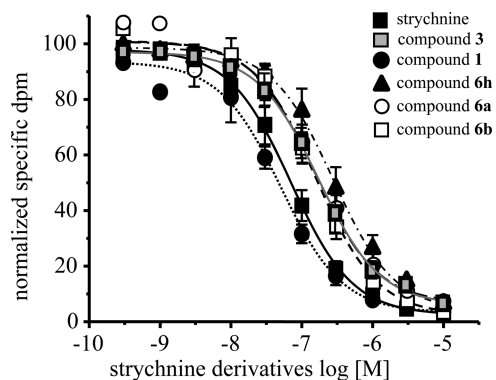


Figure 1. Displacement curves for [³H]strychnine binding experiments of compounds 1, 3, 6a, 6b, and 6h at $\alpha 1$ receptors recombinantly expressed in HEK293 cells.

are a hydrogen bond between the protonated tertiary amino group of strychnine and the backbone carbonyl group of Phe159 and a polar interaction between the lactam oxygen of strychnine and the guanidinium group of Arg65. Moreover, the protonated amino group of strychnine is also involved in an electrostatic interaction with the carboxylate group of the Glu157 side chain.

The residues essential for strychnine binding are conserved among the α and β subunits of GlyRs, with the exception that α Phe²⁰⁷ is replaced by a Tyr in the β subunit.¹⁴ Consequently, it is hardly surprising that neither strychnine nor any of the analogues in this study displayed substantial selectivity toward $\alpha 1$ or $\alpha 1\beta$ receptors. In the FMP assay, all compounds

displayed either comparable antagonist potencies at the two receptors or slightly higher potency at the homomeric receptor with 2-aminostrychnine (2) and the *n*-propyl, isobutyl, and *n*-pentyl oxime ethers 6b, 6d, and 6f, respectively, showing the highest preference toward the $\alpha 1$ subtype (3–4-fold).

While the lactam group and the C-21–C-22 double bond are present in all strychnine analogues examined in this study, two analogues lack the tertiary amino group, namely, the quaternary *n*-propyl derivative 4 and 18-oxostrychnine (5), in which N-19 is a part of a lactam function. Consequently, for both compounds, N-19 cannot exist in a protonated form required for its action as a hydrogen bond donor, which is reflected in the antagonist potencies of 4 and 5 (IC₅₀ \approx 10 μ M) being approximately 100-fold lower than those of strychnine (IC₅₀ \approx 0.1 μ M) at both $\alpha 1$ and $\alpha 1\beta$.

2-Aminostrychnine (2) has been previously identified as a high-affinity ligand for the strychnine binding sites in synaptic membranes from the brain and spinal cord of rats.¹⁵ Radioligand displacement experiments using [³H]strychnine revealed for 2 only slightly reduced affinity ($K_i = 18$ nM) when compared to strychnine ($K_i = 12$ nM).¹⁵ In the FMP assay, compound 2 exhibited strong inhibition of $\alpha 1$ (IC₅₀ = 77 nM) and $\alpha 1\beta$ (IC₅₀ = 270 nM) receptors, thus being equipotent to strychnine at both subtypes. As discussed later, docking experiments revealed that the orientation of 2-aminostrychnine in the antagonist binding pocket is highly similar to that of strychnine, with the primary amino group making an additional hydrogen bond with the backbone carbonyl group of Gly160 (Figure 2B). For the propionamide 3 (*N*-acylated 2-aminostrychnine), the *N*-acyl substituent is too bulky to be well accommodated in this region of the binding pocket, resulting in a significantly lower antagonistic potency at $\alpha 1$ (IC₅₀ = 540 nM) and $\alpha 1\beta$ (IC₅₀ = 940 nM) receptors.

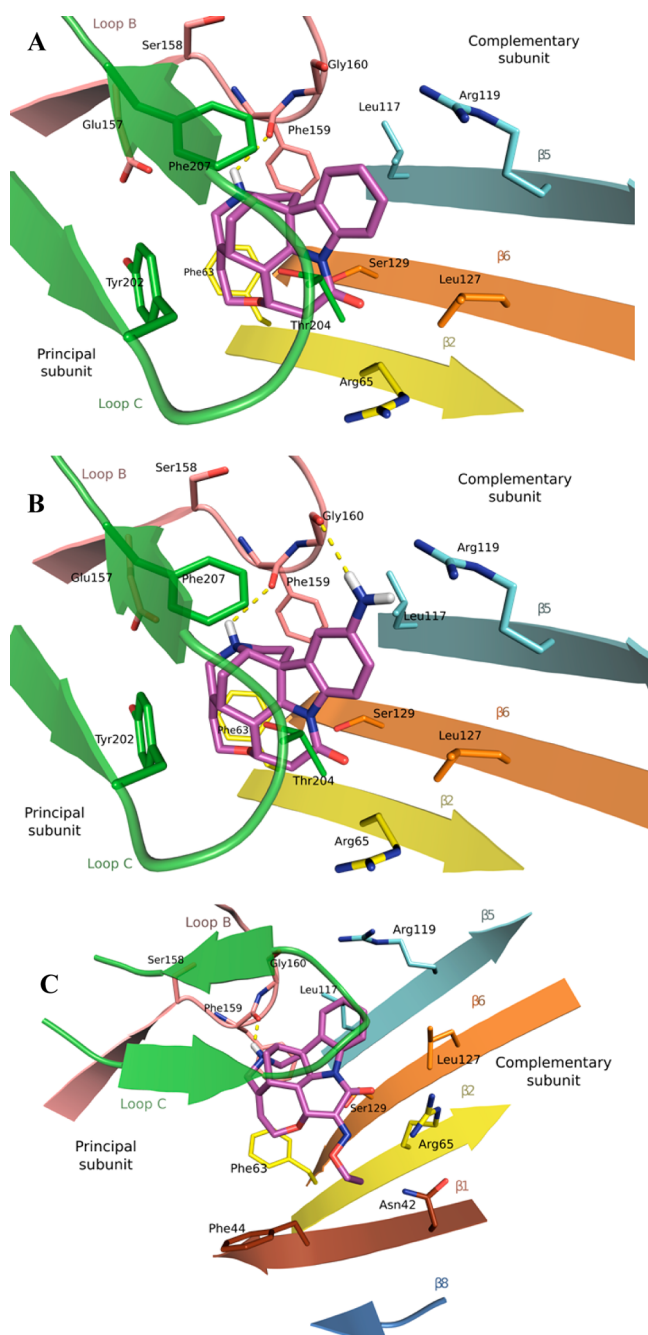


Figure 2. Graphical representation of the orthosteric binding pocket of the homomeric GlyR with docked (A) strychnine (magenta), (B) 2-aminostrychnine **2** (magenta), and (C) propargyl oxime ether **6i** (magenta), showing residues from loop B (coral) and loop C (green) of the principal subunit together with $\beta 5$ (cyan), $\beta 6$ (orange), $\beta 2$ (yellow), $\beta 1$ (brown), and $\beta 8$ (blue) from the complementary subunit. Only side chain atoms are shown for clarity.

(*E*)-11-Isonitrosostrychnine (**1**) has been previously reported to exert strong antagonistic action at GlyRs.¹⁷ In the FMP assay it displayed similar IC_{50} values ($\alpha 1$: 97 nM; $\alpha 1\beta$: 210 nM) to strychnine. An equally high inhibition was observed for its methyl ether **6a** ($\alpha 1$: IC_{50} = 100 nM; $\alpha 1\beta$: IC_{50} = 210 nM). The effect of increasing the size of the oxime ether substituent on the antagonist potency was examined in the series of ligands **6a–i**. While the *n*-propyl analogue **6b** maintained a high antagonist potency ($\alpha 1$: IC_{50} = 110 nM;

$\alpha 1\beta$: IC_{50} = 350 nM), further increasing the size of the alkyl substituent (**6c–g**, R = *n*-butyl, *iso*-butyl, benzyl, *n*-pentyl, phenethyl) gradually reduced the GlyR activity of the analogues. For example, **6g**, bearing a bulky phenethyl substituent, exhibited ~5-fold higher IC_{50} values at the GlyRs (690 nM at $\alpha 1$, 780 nM at $\alpha 1\beta$) than those of the methyl analogue **6a**. A terminal methyl ester group did not significantly change the antagonist potencies in the oxime ether series, as indicated by the IC_{50} values of the methyl acetate **6j** ($\alpha 1$: 220 nM; $\alpha 1\beta$: 720 nM) and the methyl valerate **6k** ($\alpha 1$: 720 nM; $\alpha 1\beta$: 1500 nM), the latter being less potent because of the longer spacer between the oxime ether oxygen and the ester carbonyl group.

Introduction of a double or triple bond into the propyl group of **6b** significantly improved antagonistic potency. The resulting allyl (**6h**) and propargyl (**6i**) analogues are among the most potent GlyR antagonists published to date, displaying IC_{50} values of 95 nM ($\alpha 1$) and 150 nM ($\alpha 1\beta$) and of 52 nM ($\alpha 1$) and 240 nM ($\alpha 1\beta$), respectively.

These findings indicate that the strychnine binding site at GlyRs comprises an additional lipophilic pocket located close to C-11 of strychnine, and the groups best accommodated in this pocket are (*E*)-allyl and (*E*)-propargyl oxime ethers (Figure 2C; see also later discussion of docking studies).

The analogues displaying the highest antagonist potencies in the FMP assay (**1**, **2**, **6a**, **6b**, **6h**, **6i**) and the less potent antagonists **3** and **4** were tested in whole-cell patch-clamp assays at $\alpha 1$ and $\alpha 1\beta$ GlyRs recombinantly expressed in HEK 293 cells. This method records ion-channel-mediated transmembrane currents directly and thus allows direct insight into the inhibition of GlyR function.²⁵ While the FMP assay generates an equilibrium of all receptor states (free, ligand-bound, inhibitor-bound, active, desensitized), the patch-clamp technique observes receptor activation and inhibition in a pre-equilibrium situation, where receptor desensitization, i.e., the transition into an inactive refractory state, is excluded.²⁵ The concentration-dependent reduction of GlyR currents in the presence of strychnine derivatives was used to construct concentration-inhibition curves and determine functional IC_{50} values^{26,27} (Figure S15, Supporting Information).

The IC_{50} values (Table 1) obtained in the patch-clamp recordings generally correlate well with those from the FMP assay, confirming the SAR conclusions drawn so far and indicating that the affinity of strychnine analogues for active and desensitized receptor states is similar. For most analogues, the IC_{50} values were slightly lower and none of the ligands showed preference toward the $\alpha 1$ subtype.

In order to confirm that the antagonist potencies obtained for the strychnine analogues in the two functional studies correlate with their binding affinities at the receptors, compounds **1**, **3**, **6a**, **6b**, and **6h** were subjected to radioligand binding experiments at $\alpha 1$ receptors recombinantly expressed in HEK293 cells using [³H]strychnine as radioligand. The displacement curves are shown in Figure 1. The binding affinities for the analogues (K_i values) are given in Table 2. (*E*)-11-Isonitrosostrychnine (**1**), which was found to be equipotent to strychnine in both functional assays, also exhibited comparable binding affinity (K_i = 40 nM) to the parent compound (K_i = 23 nM). 2-Propionamidostychnine (**3**), which was 3-fold less potent than strychnine in both functional assays, displayed a 3-fold decreased binding affinity (K_i = 67 nM) compared to strychnine in the binding assay. Surprisingly, the oxime ethers **6a**, **6b**, and **6h**, which exhibited antagonistic

Table 2. Binding Affinities of Compounds 1, 3, 6a, 6b, and 6h for the Human $\alpha 1$ GlyRs Expressed in HEK293 Cells Obtained in Competition Radioligand Binding Assays Using [^3H]Strychnine

	K_i [nM] \pm SEM
strychnine	23 \pm 6
1	40 \pm 4
3	67 \pm 17
6a	189 \pm 30
6b	241 \pm 67
6h	370 \pm 116

potencies similar to that of strychnine in both functional assays, showed significantly reduced binding affinity compared to the parent compound (**6a** K_i = 189 nM; **6b** K_i = 241 nM; **6h** K_i = 371 nM).

To elucidate the binding mode of the strychnine analogues, molecular docking simulation studies using GOLD 5.3 (Cambridge Crystallographic Data Centre, Cambridge, UK) were performed. Two experimentally determined structures of GlyR complexed with strychnine are available: $\alpha 1$ GlyR (PDB code: 3JAD, resolution 3.9 Å)¹³ and $\alpha 3$ GlyR (PDB code: SCFB, resolution 3.0 Å).¹⁴ Although the compounds were tested on $\alpha 1$ GlyR, the lower resolution $\alpha 1$ GlyR structure appeared to be unsuitable for docking experiments because of a missing critical side chain of Glu157 in the orthosteric binding site in addition to a flipped orientation of the backbone carbonyl group of Phe159, which made it difficult to reproduce the experimental binding mode of strychnine. Comparing the sequence of both proteins showed a high sequence identity of 89% and a sequence similarity of 95% with all orthosteric binding site residues conserved in both proteins (Figure S16, Supporting Information). Accordingly, the higher resolution crystal structure of $\alpha 3$ GlyR (SCFB) was used in this study for docking the strychnine analogues.

To validate the docking protocol, the cocrystallized ligand strychnine was docked into the orthosteric site of the glycine receptor (Figure 2A). All the resultant poses converged to a binding mode similar to that of the experimentally determined position of strychnine with the best ranking pose having a root-mean square deviation (RMSD) value of 0.36 Å (Figure S17, Supporting Information). An overlay of the docked pose and the crystal structure is shown in the Supporting Information (Figure S18). The orthosteric site is formed by Ser158, Phe159, Gly160 from loop B and Tyr202, Thr204, Phe207 from loop C of the principal unit together with Phe63, Arg65 from $\beta 2$, Leu117, Arg119 from $\beta 5$, and Leu127, Ser129 from $\beta 6$ of the complementary unit (Figure 2A).¹⁴ The binding interactions include a hydrogen bond between the protonated tertiary amine of strychnine and the backbone carbonyl group of Phe159, a polar interaction between the lactam oxygen of strychnine and the guanidinium group of Arg65, and an electrostatic interaction of the protonated amino group of strychnine with the carboxylate group of the Glu157 side chain. Moreover, the benzene rings of Phe159, Phe207, and Phe63 are involved in hydrophobic interactions with hydrophobic parts of the strychnine molecule, such as the methylene groups CH₂-17 and CH₂-18 and the C-21–C-22 double bond.

2-Aminostrychnine (**2**) was equipotent to strychnine in both functional assays. Docking studies revealed that **2** fitted very well into the orthosteric site of the $\alpha 3$ GlyR with the same orientation and interactions of the strychnine skeleton as for

the parent compound (Figure 2B). The primary amino group is involved in a hydrogen bond with the backbone carbonyl of Gly₁₆₀ of the principal subunit.

As for the oxime ethers, the strychnine core adopted a similar orientation in the orthosteric site of the $\alpha 3$ GlyR when compared to strychnine. As shown for the most potent propargyl oxime ether, **6i** (Figure 2C), the propargyl group protrudes into a groove of a limited size flanked from one end by Phe44 and Phe63, while the other end is lined by Arg65 and Asn42 belonging to the $\beta 1$ and $\beta 2$ strands of the complementary subunit. On the other hand, for the least potent oxime ether, **6g**, bearing a phenethyl group, the bulky phenyl ring fails to fit into this confined area, shifting the substituent toward the $\beta 8$ strand (Figure S19, Supporting Information).

In summary, a series of (*E*)-11-isonitrosostrychnine oxime ethers were synthesized and characterized as antagonists at homomeric and heteromeric glycine receptors in the FMP assay, in a whole-cell patch-clamp assay, and in [^3H]strychnine binding studies. The most potent antagonists in the series bear methyl, allyl, and propargyl substituents. While the methyl and allyl analogues **6a** and **6h** were equipotent to strychnine, the propargyl oxime ether **6i** was a slightly more potent antagonist than the parent compound. Docking studies to the strychnine binding site from the crystal structure of the $\alpha 3$ GlyR revealed the presence of a hydrophobic region that is able to accommodate small oxime ether substituents. The findings provide a valuable extension of the SAR of strychnine at the $\alpha 1$ and $\alpha 1\beta$ receptors and reveal the oxime ether group as a possible linker for strychnine-based bivalent ligands targeting glycine receptors, which currently are under investigation in our laboratories.

EXPERIMENTAL SECTION

General Experimental Procedures. Melting points were determined using a capillary melting point apparatus (Gallenkamp, Sanyo) and are uncorrected. A Bruker AV-400 spectrometer was used to obtain ^1H NMR and ^{13}C NMR spectra, respectively. ^1H NMR chemical shifts are referred to CHCl₃ (7.26 ppm) and DMSO-*d*₆ (2.50 ppm). ^{13}C NMR chemical shifts are referred to CDCl₃ (77.26 ppm) and DMSO-*d*₆ (39.52 ppm). The NMR resonances were assigned by means of COSY and HMQC experiments. ESI mass spectra were determined on an Agilent 1100 MS system. Elemental analyses were performed by the microanalytical section of the Institute of Inorganic Chemistry, University of Würzburg. All reactions were carried out under an argon atmosphere. Column chromatography was carried out on silica gel 60 (0.063–0.200 mm) obtained from Merck (Darmstadt, Germany). 2-Aminostrychnine (**2**) was synthesized by nitration of strychnine and reduction of the resulting 2-nitrostrychnine using SnCl₂.²⁰ *N*-Propylstrychnine bromide (**4**) was prepared as previously described.²¹

***N*-(Strychnin-2-yl)propionamide (3).** Propionic anhydride (4.4 mL) was dropwise added to the solution of 2-aminostrychnine (290 mg, 0.83 mmol) and Et₃N (2.53 mL) in dry CH₂Cl₂ (20 mL). After stirring for 2 h at room temperature, the solvent was removed under reduced pressure and the residue was subjected to column chromatography (CHCl₃–MeOH–25% NH₃, 100:10:1) to give **3** (256 mg, 76%) as a colorless solid: ^1H NMR (400 MHz, CDCl₃) δ 7.99 (1H, d, *J* = 8.6 Hz, H-4), 7.60 (1H, d, *J* = 1.9 Hz, H-1), 7.42 (1H, s, NH), 7.14 (1H, dd, *J* = 8.6, 1.9 Hz, H-3), 5.87 (1H, t, *J* = 6.0 Hz, H-2), 4.26 (1H, dt, *J* = 8.4, 3.3 Hz, H-12), 4.13 (1H, dd, *J* = 13.8, 6.9 Hz, H-23a), 4.04 (1H, dd, *J* = 13.8, 6.0 Hz, H-23b), 3.92 (1H, s, H-16), 3.84 (1H, d, *J* = 10.5 Hz, H-8), 3.67 (1H, dd, *J* = 14.8, 1.0 Hz, H-20a), 3.19–3.06 (3H, m, H-11a, H-14, H-18a), 2.83 (1H, td, *J* = 10.1, 7.7 Hz, H-18b), 2.72–2.60 (2H, m, H-11b, H-20b), 2.37 (2H, q, *J* = 7.5 Hz, –CH₂CH₃), 2.34–2.28 (1H, m, H-17a), 1.95–1.81 (2H, m,

H-15a, H-15b), 1.42 (1H, d, $J = 14.4$ Hz, H-17b), 1.25–1.22 (1H, m, H-13), 1.23 (3H, t, $J = 7.5$ Hz, $-\text{CH}_2\text{CH}_3$); ^{13}C NMR (100 MHz, CDCl_3) δ 171.76 (C, C=O), 168.92 (C, C-10), 140.42 (C, C-5), 138.36 (C, C-21), 134.51 (C, C-6), 133.59 (C, C-2), 126.93 (CH, C-22), 119.83 (CH, C-3), 116.12 (CH, C-4), 114.40 (CH, C-1), 77.45 (CH, C-12), 64.43 (CH₂, C-23), 60.21 (CH, C-16), 59.91 (CH, C-8), 52.51 (CH₂, C-20), 51.88 (C, C-7), 50.13 (CH₂, C-18), 48.03 (CH, C-13), 42.56 (CH₂, C-15), 42.17 (CH₂, C-11), 31.40 (CH, C-14), 30.45 (CH₂, $-\text{CH}_2\text{CH}_3$), 26.71 (CH₂, C-17), 9.50 (CH₃, $-\text{CH}_2\text{CH}_3$); ESIMS m/z 405.8 $[\text{M}]^+$ (100%); *anal.* C 71.00, H 6.86, N 10.15%, calcd for $\text{C}_{24}\text{H}_{27}\text{N}_3\text{O}_3$ C 71.09, H 6.71, N 10.36%.

18-Oxostrychnine (5). A solution of $\text{K}_2\text{Cr}_2\text{O}_7$ (6 mg, 0.02 mmol) in 2 mL of H_2O was added to a solution of strychnine *N*-oxide (200 mg, 0.57 mmol) in 10 mL of H_2O and 5 mL of dioxane, and the reaction mixture was heated under reflux for 2 h. After cooling to room temperature, the solvent was removed under reduced pressure. Water (4 mL) and warm (45 °C) 1 N HCl (10 mL) were added to the residue, and the insoluble brown material was filtered off and subjected to column chromatography (CH_2Cl_2 -MeOH-25% NH_3 , 100:5:0.5) to give compound **5** (70 mg, 35.3%) as a colorless solid: mp 263 °C (lit. 263 °C); ^1H NMR (400 MHz, CDCl_3) δ 8.09–8.01 (1H, m, H-4), 7.82 (1H, dd, $J = 7.8, 0.9$ Hz, H-1), 7.23–7.15 (1H, m, H-3), 7.00 (1H, dd, $J = 5.1, 2.5$ Hz, H-2), 5.88 (1H, t, $J = 6.2$ Hz, H-22), 4.21 (1H, dt, $J = 8.4, 3.6$ Hz, H-12), 4.09 (1H, dd, $J = 13.9, 6.9$ Hz, H-23a), 3.98 (1H, dd, $J = 13.9, 6.1$ Hz, H-23b), 3.85 (1H, dd, H-20a), 3.77 (1H, d, $J = 10.6$ Hz, H-8), 3.20 (1H, d, $J = 11.0$ Hz, H-14), 3.18–3.13 (1H, m, H-18a), 3.08–3.00 (1H, m, H-11a), 2.85–2.72 (2H, m, H-18b, H-20b), 2.57 (1H, dd, $J = 17.4, 3.6$ Hz, H-11b), 2.301–2.162 (2H, m, H-15a, H-17a), 1.831–1.680 (2H, m, H-15b, H-17b), 1.31 (1H, ddd, $J = 13.0, 8.2, 4.8$ Hz, H-13); ^{13}C NMR (101 MHz, CDCl_3) δ 170.3 (C, C=O), 169.0 (C, C-10), 142.0 (C, C-5), 138.9 (C, C-21), 131.8 (C, C-6), 128.7 (CH, C-2), 127.4 (CH, C-3), 124.3 (CH, C-22), 115.7 (CH, C-4), 92.5 (C, C-16), 77.3 (CH, C-12), 65.2 (CH₂, C-23), 60.4 (CH, C-8), 56.6 (C, C-7), 52.8 (CH₂, C-20), 48.7 (CH, C-13), 48.4 (CH₂, C-18), 42.7 (CH₂, C-11), 39.8 (CH₂, C-17), 35.0 (CH₂, C-15), 33.4 (CH, C-14); ESIMS $m/z = 350.2$ $[\text{M}]^+$.

General Procedure for the Synthesis of the Oxime Ethers 6a–k. A solution of **1** (500 mg, 1.4 mmol) in dry DMF (4 mL) was added dropwise to a stirred suspension of NaH (0.03 g, 1.4 mmol, 60% dispersion in mineral oil) in dry DMF (3 mL) at 0 °C. After stirring at 0 °C for 30 min, the respective alkyl halide (0.32 mmol) was dropwise added. After stirring at room temperature for 16 h, the mixture was concentrated under reduced pressure and the residue was subjected to column chromatography using CH_2Cl_2 -MeOH-25% NH_3 (100:5:0.5) as eluent unless otherwise stated.

(E)-11-(Methoxyimino)strychnine (6a). **6a** (60 mg, 12%) was obtained from **1** and CH_3I (0.02 mL) as a pale yellow solid: ^1H NMR (400 MHz, $\text{DMSO}-d_6$) δ 8.03 (1H, d, $J = 7.7$ Hz, H-4), 7.39 (1H, d, $J = 7.0$ Hz, H-2), 7.34–7.28 (1H, m, H-3), 7.17 (1H, td, $J = 7.5, 0.9$ Hz, H-1), 5.73 (1H, t, $J = 4.9$ Hz, H-22), 4.85 (1H, d, $J = 2.4$ Hz, H-12), 4.092–4.013 (2H, m, H-23a, H-23b), 3.97 (3H, s, CH_3), 3.93 (1H, d, $J = 10.8$ Hz, H-8), 3.80 (1H, dd, $J = 12.1$ Hz, H-16), 3.49 (1H, d, $J = 14.2$ Hz, H-20a), 2.96–2.96 (1H, m, H-14), 2.93–2.87 (1H, m, H-18a), 2.63–2.57 (1H, m, H-18b), 2.50 (1H, d, $J = 14.2$ Hz, H-20b), 2.26–2.14 (1H, m, H-15a), 1.79 (1H, m, H-17a), 1.64–1.57 (1H, m, H-13), 1.51 (ddd, $J = 10.8, 2.6$ Hz, H-17b), 1.27 (1H, ddd, $J = 14.3$ Hz, H-15b); ^{13}C NMR (100 MHz, $\text{DMSO}-d_6$) δ 158.2 (C, C=O), 149.5 (C, C=N), 142.2 (C, C5), 140.4 (C, C21), 134.1 (C, C6), 128.2 (CH, C-3), 126.6 (CH, C-22), 124.6 (CH, C-1), 122.8 (CH, C-2), 114.8 (CH, C-4), 75.4 (CH, C-12), 65.3 (CH₂, C-23), 63.6 (CH₃, O- CH_3), 59.5 (CH, C-16), 58.8 (CH, C-8), 52.4 (CH₂, C-20), 51.2 (C, C7), 49.4 (CH₂, C-18), 44.5 (CH, C-13), 42.8 (CH₂, C-17), 31.3 (CH, C-14), 26.4 (CH₂, C-15); ESIMS m/z 377.6 $[\text{M}]^+$; mp 181 °C; *anal.* C 69.42, H 6.30, N 10.64%, calcd for $\text{C}_{22}\text{H}_{23}\text{N}_3\text{O}_3 \times 1/3\text{MeOH}$ C 69.11, H 6.32, N 10.83%.

(E)-11-(Propyloxyimino)strychnine (6b). **6b** (130 mg, 25%) was obtained from **1** and *n*-propyl bromide (0.03 mL) in the presence of KI (1 mg) as a white solid: ^1H NMR (400 MHz, $\text{DMSO}-d_6$) δ 4.28 (2H, t, $J = 6.4$ Hz, $\text{OCH}_2\text{CH}_2\text{CH}_3$), 1.74 (2H, m, $\text{OCH}_2\text{CH}_2\text{CH}_3$), 0.99 (3H, t, $J = 7.4$ Hz, $-\text{OCH}_2\text{CH}_2\text{CH}_3$); δ and J values for all other

hydrogen atoms coincide with the values for the corresponding atoms of **6a** within ± 0.04 ppm and ± 0.1 Hz, respectively; ^{13}C NMR (100 MHz, $\text{DMSO}-d_6$) 77.0 ($\text{OCH}_2\text{CH}_2\text{CH}_3$), 22.1 ($\text{OCH}_2\text{CH}_2\text{CH}_3$), 10.0 (CH_3 , $\text{OCH}_2\text{CH}_2\text{CH}_3$); chemical shifts for all other carbon atoms coincide with the δ values for the corresponding atoms of **6a** within ± 0.1 ppm; ESIMS m/z 405.4 $[\text{M}]^+$; mp 182 °C; *anal.* C 69.63, H 6.41, N 9.98%, calcd for $\text{C}_{24}\text{H}_{27}\text{N}_3\text{O}_3 \times 0.5\text{MeOH}$ C 69.81, H 6.93, N 9.97%.

(E)-11-(Butyloxyimino)strychnine (6c). **6c** (40 mg, 7.3%) was obtained from **1** and *n*-butyl bromide (0.03 mL) in the presence of KI (1 mg) as a brown solid: ^1H NMR (400 MHz, CDCl_3) δ 8.17 (1H, d, $J = 8.0$ Hz, H-3), 8.00 (1H, s, H-1), 7.30–7.23 (1H, m, H-4), 7.11 (1H, t, $J = 7.1$ Hz, H-2), 5.89 (1H, s, H-22), 4.95 (1H, d, $J = 2.4$ Hz, H-12), 4.46–4.36 (2H, m, $\text{OCH}_2(\text{CH}_2)_2\text{CH}_3$), 4.28 (1H, dd, $J = 13.9, 7.1$ Hz, H-23a), 4.17 (1H, d, $J = 10.6$ Hz, H-8), 4.11 (1H, dd, $J = 12.9, 5.7$ Hz, H-23b), 3.96 (1H, s, H-16), 3.70 (1H, d, $J = 14.6$ Hz, H-20a), 3.14 (1H, dd, $J = 16.8, 8.2$ Hz, H-18a), 3.06 (1H, s, H-14), 2.84 (1H, d, $J = 5.0$ Hz, H-18b), 2.68 (1H, d, $J = 14.6$ Hz, H-20b), 2.39 (1H, dt, $J = 14.4, 4.2$ Hz, H-15a), 1.92–1.85 (2H, m, H-17), 1.79–1.70 (2H, m, $\text{OCH}_2\text{CH}_2\text{CH}_2\text{CH}_3$), 1.56–1.38 (4H, m, $\text{O}(\text{CH}_2)_2\text{CH}_2\text{CH}_3$, H-13, H-15b), 0.99–0.90 (3H, m, CH_3); ^{13}C NMR (101 MHz, CDCl_3) δ 159.2 (C, C=O), 149.5 (C, C=N), 142.7 (C, C-5), 139.5 (C, C-21), 133.1 (C, C-6), 129.4 (C, C-3), 127.4 (CH, C-22), 125.2 (C, C-1), 122.1 (C, C-4), 116.6 (C, C-1), 77.3 (CH_2 , $\text{OCH}_2(\text{CH}_2)_2\text{CH}_3$), 76.3 (CH, C-12), 66.5 (CH₂, C-23), 60.1 (CH, C-16), 58.6 (CH, C-8), 53.5 (C, C-7), 52.8 (CH₂, C-20), 49.9 (CH₂, C-18), 45.8 (CH, C-13), 43.3 (CH₂, C-17), 32.8 (CH, C-14), 30.6 (CH₂, $\text{CH}_2\text{CH}_2\text{CH}_2\text{CH}_3$), 27.1 (CH₂, C-15), 19.5 (CH₃, $\text{O}(\text{CH}_2)_2\text{CH}_2\text{CH}_3$), 14.1 (CH₃, CH_3); ESIMS m/z 419.4 $[\text{M}]^+$; mp 121 °C; *anal.* C 71.32, H 6.52, N 9.72%, calcd for $\text{C}_{25}\text{H}_{29}\text{N}_3\text{O}_3$ C 71.58, H 6.97, N 10.02%.

(E)-11-(Isobutyloxyimino)strychnine (6d). **6d** (30 mg, 5.5%) was obtained from **1** and 1-bromo-2-methylpropane (0.04 mL) in the presence of KI (1 mg) as a white solid: ^1H NMR (400 MHz, CDCl_3) δ 4.13–4.08 [2H, m, $\text{OCH}_2\text{CH}(\text{CH}_3)_2$], 2.02 [1H, m, $\text{OCH}_2\text{CH}(\text{CH}_3)_2$], 0.91 [6H, dd, $J = 6.6, 5.8$ Hz, $\text{OCH}_2\text{CH}(\text{CH}_3)_2$], δ and J values for all other hydrogen atoms coincide with the values for the corresponding atoms of **6c** within ± 0.04 ppm and ± 0.1 Hz, respectively; ^{13}C NMR (100 MHz, CDCl_3) δ 83.0 (CH_2 , $\text{OCH}_2\text{CH}(\text{CH}_3)_2$), 28.7 (CH, $\text{OCH}_2\text{CH}(\text{CH}_3)_2$), 19.2 (CH_3 , $\text{OCH}_2\text{CH}(\text{CH}_3)_2$); chemical shifts for all other carbon atoms coincide with the δ values for the corresponding atoms of **6c** within ± 0.1 ppm; ESIMS m/z 419.5 $[\text{M}]^+$; mp 121 °C; *anal.* C 71.42, H 6.66, N 9.78%, calcd for $\text{C}_{25}\text{H}_{29}\text{N}_3\text{O}_3$ C 71.58, H 6.97, N 10.02%.

(E)-11-(Benzyloxyimino)strychnine (6e). **6e** (45 mg, 9%) was obtained from **1** and benzyl bromide (0.04 mL) as a white solid; eluate for column chromatography CH_2Cl_2 -MeOH (100:7): ^1H NMR (400 MHz, CDCl_3) δ 7.43–7.32 (5H, m, $\text{CH}_2\text{C}_6\text{H}_5$), 5.57 (1H, d, $J = 12.3$ Hz, HCHC_6H_5), 5.43 (1H, d, $J = 12.3$ Hz, HCHC_6H_5); δ and J values for all other hydrogen atoms coincide with the values for the corresponding atoms of **6c** within ± 0.04 ppm and ± 0.1 Hz, respectively; ^{13}C NMR (100 MHz, CDCl_3) δ 136.9 (C, CH_2C_{ar}), 128.7 (CH, $2 \times \text{CH}_2\text{CCH}_{ar}$), 128.2 (C, $\text{CH}_2\text{CCHCH}_{ar}$), 128.1 (CH, $2 \times \text{CH}_2\text{CCH}_{ar}$); chemical shifts for all other carbon atoms coincide with the δ values for the corresponding atoms of **6c** within ± 0.1 ppm; ESIMS m/z 453.4 $[\text{M}]^+$; mp 144 °C; *anal.* C 73.53, H 5.88, N 8.77%, calcd for $\text{C}_{28}\text{H}_{27}\text{N}_3\text{O}_3 \times 1/3\text{MeOH}$ C 73.31, H 6.15, N 9.05%.

(E)-11-(Pentyloxyimino)strychnine (6f). **6f** (100 mg, 18%) was obtained from **1** and *n*-pentyl bromide (0.04 mL) in the presence of KI (1 mg) as a white solid: ^1H NMR (400 MHz, CDCl_3) δ 4.43–4.32 [2H, m, $\text{OCH}_2(\text{CH}_2)_3\text{CH}_3$], 1.73 [2H, m, $\text{OCH}_2\text{CH}_2(\text{CH}_2)_2\text{CH}_3$], 1.40–1.31 [4H, m, $\text{OCH}_2\text{CH}_2(\text{CH}_2)_2\text{CH}_3$], 0.92–0.86 [3H, m, $\text{O}(\text{CH}_2)_4\text{CH}_3$]; δ and J values for all other hydrogen atoms coincide with the values for the corresponding atoms of **6c** within ± 0.04 ppm and ± 0.1 Hz, respectively; ^{13}C NMR (100 MHz, CDCl_3) δ 76.9 (CH_2 , $\text{OCH}_2(\text{CH}_2)_3\text{CH}_3$), 29.0 [CH_2 , $\text{OCH}_2\text{CH}_2(\text{CH}_2)_2\text{CH}_3$], 28.1 [CH_2 , $\text{O}(\text{CH}_2)_2\text{CH}_2\text{CH}_2\text{CH}_3$], 22.4 [CH_2 , $\text{O}(\text{CH}_2)_3\text{CH}_2\text{CH}_3$], 14.1 (CH_3 , CH_3); chemical shifts for all other carbon atoms coincide with the δ values for the corresponding atoms of **6c** within ± 0.1 ppm; ESIMS m/z

z 433.5 [M]⁺; mp 109 °C; anal. C 73.53, H 5.88, N 8.77%, calcd for C₂₆H₃₁N₃O₃ C 73.40, H 5.80, N 8.69%.

(*E*)-11-[(Phenylethyl)imino]strychnine (**6g**). **6g** (33 mg, 6%) was obtained from **1** and 2-phenylethyl bromide (0.044 mL) as a white solid; eluate for column chromatography CH₂Cl₂–MeOH (100:7): ¹H NMR (400 MHz, CDCl₃) δ 7.30–7.09 (5H, m, CH₂C₆H₅), 4.69–4.55 (2H, m, OCH₂CH₂C₆H₅), 3.12–3.04 (2H, m, OCH₂CH₂C₆H₅); δ and J values for all other hydrogen atoms coincide with the values for the corresponding atoms of **6c** within ±0.02 ppm and ±0.1 Hz, respectively; ¹³C NMR (100 MHz, CDCl₃) δ 138.6 (C, CH₂C_{ar}), 129.3 (CH, 2 × CH₂CCH_{ar}), 129.2 (C, CH₂CCHCH_{ar}), 128.6 (CH, 2 × CH₂CCHCH_{ar}); 77.6 (CH₂, OCH₂CH₂C₆H₅), 35.7 (CH₂, OCH₂CH₂C₆H₅); chemical shifts for all other carbon atoms coincide with the δ values for the corresponding atoms of **6c** within ±0.1 ppm; ESIMS *m/z* 467.6 [M]⁺; mp 189 °C; anal. C 73.74, H 6.61, N 8.58%, calcd for C₂₉H₂₉N₃O₃ × 1/3MeOH, C 73.67, H 6.39, N 8.79%.

(*E*)-11-(Allyloxyimino)strychnine (**6h**). **6h** (45 mg, 9%) was obtained from **1** and allyl bromide (0.03 mL) as a pale yellow solid: ¹H NMR (400 MHz, CDCl₃) δ 6.10–6.00 (1H, m, CH=CH₂), 5.39 (1H, ddd, *J* = 17.3, 3.2, 1.6 Hz, CH=CHH), 5.27 (1H, dd, *J* = 10.5, 1.4 Hz, CH=CHH), 4.98–4.86 (2H, m, CH₂CH=CH₂); δ and J values for all other hydrogen atoms coincide with the values for the corresponding atoms of **6c** within ±0.04 ppm and ±0.1 Hz, respectively; ¹³C NMR (100 MHz, CDCl₃) δ 133.2 (CH, CH=CH₂), 118.6 (CH₂, CH=CH₂), 77.9 (CH₂, CH₂CH=CH₂); chemical shifts for all other carbon atoms coincide with the δ values for the corresponding atoms of **6c** within ±0.1 ppm; ESIMS *m/z* 402.4 [M – 1]⁺; mp 161 °C; anal. C 70.42, H 6.30, N 9.70%, calcd for C₂₄H₂₅N₃O₃ × 1/3MeOH, C 70.57, H 6.41, N 10.15%.

(*E*)-11-(Propargyloxyimino)strychnine (**6i**). **6i** (130 mg, 25%) was obtained from **1** and propargyl chloride (0.023 mL) in the presence of KI (1 mg) as a pale brown solid: ¹H NMR (400 MHz, CDCl₃) δ 4.95–4.92 (3H, m, CH₂C≡CH, H-12), 2.47 (1H, t, *J* = 2.4 Hz, C≡CH); δ and J values for all other hydrogen atoms coincide with the values for the corresponding atoms of **6c** within ±0.04 ppm and ±0.1 Hz, respectively; ¹³C NMR (100 MHz, CDCl₃) δ 78.5 (CH, C≡CH), 63.9 (CH₂, CH₂C≡CH); chemical shifts for all other carbon atoms coincide with the δ values for the corresponding atoms of **6c** within ±0.1 ppm; ESIMS *m/z* 401.4 [M]⁺; mp 148 °C; anal. C 71.42, H 6.12, N 10.06%, calcd for C₂₄H₂₃N₃O₃, C 71.80, H 5.77, N 10.47%.

(*E*)-11-[(Methoxycarbonylmethyl)oxyimino]strychnine (**6j**). **6j** (130 mg, 23%) was obtained from **1** and methyl bromoacetate (0.03 mL) as a pale brown solid: ¹H NMR (400 MHz, CDCl₃) δ 4.99 (1H, d, *J* = 16.5 Hz, CHHCO₂CH₃), 4.90 (1H, d, *J* = 16.5 Hz, CHHCO₂CH₃), 3.74 (3H, s, OCH₃); δ and J values for all other hydrogen atoms coincide with the values for the corresponding atoms of **6c** within ±0.02 ppm and ±0.1 Hz, respectively; ¹³C NMR (100 MHz, CDCl₃) δ 169.3 (C, COOCH₃), 72.2 (CH₂, CH₂CO₂CH₃), 52.2 (CH₃, OCH₃); chemical shifts for all other carbon atoms coincide with the δ values for the corresponding atoms of **6c** within ±0.1 ppm; ESIMS *m/z* 435.4 [M]⁺; mp 233 °C; anal. C 65.48, H 6.24, N 9.58%, calcd for C₂₄H₂₅N₃O₅ × 1/3MeOH, C 65.51, H 5.95, N 9.42%.

(*E*)-11-[(Methoxycarbonylbutyl)oxyimino]strychnine (**6k**). **6k** (100 mg, 16%) was obtained from **1** and methyl 5-bromovalerate (0.05 mL) as a white solid: ¹H NMR (400 MHz, CDCl₃) δ 4.42–4.30 [2H, m, OCH₂(CH₂)₃CO₂CH₃], 3.64 (3H, s, OCH₃), 2.39–2–33 [2H, m, O(CH₂)₃CH₂CO₂CH₃], 1.78–1.72 [2H, m, OCH₂CH₂(CH₂)₂CO₂CH₃], 1.48–1.44 [2H, m, O(CH₂)₃CH₂CO₂CH₃]; δ and J values for all other hydrogen atoms coincide with the values for the corresponding atoms of **6c** within ±0.02 ppm and ±0.1 Hz, respectively; ¹³C NMR (100 MHz, CDCl₃) δ 174.0 (C, COOCH₃), 76.9 [CH₂, OCH₂(CH₂)₃CO₂CH₃], 51.5 (CH₃, OCH₃), 43.4 [CH₂, O(CH₂)₃CH₂CO₂CH₃], 27.2 [OCH₂CH₂(CH₂)₂CO₂CH₃], 21.5 [CH₂, O(CH₂)₃CH₂CO₂CH₃]; chemical shifts for all other carbon atoms coincide with the δ values for the corresponding atoms of **6c** within ±0.1 ppm; ESIMS *m/z* 477.5 [M]⁺; mp 115 °C; anal. C 67.81, H 6.43, N 9.58%, calcd for C₂₄H₂₅N₃O₅, C 67.91, H 6.54, N 9.48%.

FLIPR Membrane Potential Blue Assay. The functional characterization of the strychnine analogues was performed in the

FLIPR membrane potential blue assay (Molecular Devices, USA).²³ The tsA201 cells were maintained in Dulbecco's modified Eagle medium + Glutamax-I, supplemented with 10% fetal bovine serum (FBS), 100 units/mL penicillin, and 100 μg/mL streptomycin at 37 °C in a humidified 5% CO₂ atmosphere. The cells were split into 10 cm (2 × 10⁶ cells) tissue culture plates and transfected the following day with a total of 8 μg of cDNA using Polyfect transfection reagent according to the protocol of the manufacturer (Qiagen, Hilden, Germany). The following day, the cells were split into poly-D-lysine-coated black 96-well plates with a clear bottom (BD Biosciences, Bedford, MA, USA). Sixteen to 24 h later the medium was aspirated, and the cells were washed with 100 μL of Krebs buffer [140 mM NaCl/4.7 mM KCl/2.5 mM CaCl₂/1.2 mM MgCl₂/11 mM HEPES/10 mM D-glucose, pH 7.4]. Then 50 μL of Krebs buffer was added to the wells (in the antagonist experiments, various concentrations of the antagonist were dissolved in the buffer), and an additional 50 μL of Krebs buffer supplemented with the FMP assay dye (1 mg/mL) was added to each well. The plate was incubated at 37 °C in a humidified 5% CO₂ incubator for 30 min and assayed in a FlexStation3 benchtop multimode microplate reader (Molecular Devices) measuring emission at 565 nm (in fluorescence units) caused by excitation at 525 nm a total of 90 s before and after addition of 33 μL of agonist solution in Krebs buffer. The experiments were performed in duplicate at least three times for each compound at each receptor using an EC₅₀ (EC₄₀–EC₆₀) concentration of glycine as agonist.

Single-Cell Patch-Clamp Assay. The direct activity of strychnine derivatives on GlyR ion channel function was assessed using whole-cell patch-clamp recording techniques. HEK293 cells were grown in 10 cm tissue culture Petri dishes in MEM (Sigma, Deisenhofen, Germany) supplemented with 10% FBS (Invitrogen, Karlsruhe, Germany) and 5000 IU penicillin/streptomycin at 5% CO₂ and 37 °C in a water-saturated atmosphere. For experiments, cells were plated on poly-L-lysine-treated glass coverslips in 6 cm dishes. Transfection with human GlyR alpha1 and beta subunits, each in the pRK5 vector, was performed 1 day after cell passage using Gen-Carrier (Epoch Lifesciences, Sugarland, TX, USA): 1.3 μg of receptor cDNA, 1.3 μg of green fluorescence protein cDNA, and 2.6 μL of GenCarrier were used, following the manufacturer's instructions. Measurements were performed 2 to 4 days after transfection.

Current responses from GlyR-transfected HEK293 cells were measured at room temperature (21–23 °C) at a holding potential of –50 mV. Whole-cell recordings were performed using a HEKA EPC10 amplifier (HEKA Electronics, Lambrecht, Germany) controlled by Pulse software (HEKA Electronics). Recording pipets were pulled from borosilicate glass tubes (World Precision Instruments, Berlin, Germany) using a Sutter P-97 horizontal puller (Sutter, Novato, CA, USA). Solutions were applied using an Octaflow system (NPI Electronics, Tamm, Germany), where cells were bathed in a laminar flow of buffer, giving a time resolution for solution exchange and re-equilibration of about 100 ms. The external buffer consisted of 135 mM NaCl, 5.5 mM KCl, 2 mM CaCl₂, 1.0 mM MgCl₂, and 10 mM Hepes (pH adjusted to 7.4 with NaOH); the internal buffer was 140 mM CsCl, 1.0 mM CaCl₂, 2.0 mM MgCl₂, 5.0 mM EGTA, and 10 mM Hepes (pH adjusted to 7.2 with CsOH). Dose–response curves for GlyR activation by glycine were calculated from a fit to the Hill equation $\frac{I_{\text{glycine}}}{I_{\text{sat}}} = \frac{[\text{Glycine}]^{n_{\text{Hill}}}}{[\text{Glycine}]^{n_{\text{Hill}}} + \text{EC}_{50}^{n_{\text{Hill}}}}$ using a nonlinear algorithm in Microcal Origin (Additive, Friedrichsdorf, Germany). Here, I_{glycine} is the current amplitude at a given glycine concentration, I_{sat} is the maximum current amplitude at saturating concentrations of glycine, EC_{50} is the glycine concentration at half-maximal current responses, and n_{Hill} is the Hill coefficient. Currents from each individual cell were normalized to the maximum response at saturating glycine concentrations. Inhibition curves were determined from varying the concentration of strychnine derivatives in the presence of glycine near EC_{50} , i.e., 40 μM glycine for α1 receptors and 50 μM glycine for α1β receptors using 4 to 7 cells per each inhibitor. IC₅₀ values were determined from inhibition curves that were constructed using a nonlinear fit to the equation $I_{\text{obs}} = I_{\text{max}}/[1 + ([I]/\text{IC}_{50})]$, where I_{obs} is the observed current at any given concentration of inhibitor, I_{max} is the

maximum current amplitude observed in the absence of inhibitor, and [I] is the concentration of inhibitor. In all experiments EC₅₀ values were determined for each individual cell from a nonlinear fit of dose response data to the logistic equation (above). All data are given as means ± SEM.

Radioligand Binding Studies. Cell Line and Transfection. Transiently transfected tsA201 (=HEK293) cells in Dulbecco's modified Eagle medium + Glutamax-I (2 mM), supplemented with 10% fetal bovine serum, 1 mM sodium pyruvate, and 1% Pen/Strep at 37 °C in a humidified 5% CO₂ atmosphere were used for the experiments. Cells were transfected with a modified Ca₃(PO₄)₃ precipitation method (10 μg plasmid GlyRα1 DNA, 50 μL of 2.5 M CaCl₂, 440 μL of 0.1× TE-buffer, 500 μL of HBS-transfection buffer (50 mM HEPES, 12 mM dextrose, 10 mM KCl, 28 mM NaCl, 1.5 mM Na₂HPO₄, pH 6.95), mixed, incubated for 20 min at room temperature, dropwise given to cells) and washed with medium 12 h post-transfection. Following 48 h post-transfection, cells were harvested.

Membrane Protein Preparation. Cell pellets from transfected cells were homogenized in K₃PO₄ buffer (buffer H = 10 mM K₃PO₄, pH 7.4, protease inhibitor tablet complete, Roche, Mannheim, Germany). Following homogenization, the protein suspension was centrifuged at 30000g for 20 min. After a repeating step of homogenization and centrifugation, the membrane pellet was resuspended in buffer B (25 mM K₃PO₄, 200 mM KCl). GlyRα1 expression was verified using immunostaining with a pan-α antibody following Western blotting.

Radioligand Binding Assay. GlyR protein (80 μg) was used for sample preparation in a radioligand binding assay. In order to determine the binding affinities of the strychnine analogues, all compounds were diluted to concentrations of 10 000, 3000, 1000, 300, 100, 30, 10, 1, and 0.3 nM and incubated with 80 μg of GlyR protein for 30 min on ice (all data points were done in triplicates). [³H] strychnine (9.6 nM) was added and incubated with the suspension for an additional 30 min on ice. The suspension was filtered through GC/F glass microfiber filters (preincubated in buffer B + 0.5% BSA) and washed twice with buffer B, dried, and resuspended in scintillation liquid. All samples were analyzed in a Tri-Carb liquid scintillation counter (PerkinElmer, Rodgau, Germany).

Molecular Modeling. The crystal structure of the human glycine receptor α3 bound to strychnine (PDB code: 5CFB)¹⁴ was downloaded from the PDB database. The protein was prepared with the structure preparation wizard in MOE (version 2015.10²⁸) and saved as a mol2 file. The 3D structures of compounds **1**, **2**, **6i**, and **6g** were built based on the X-ray crystallographic structure of strychnine.²⁹ The compounds were minimized using the MMFF94x force field in MOE using a gradient of 0.0001 kcal/(mol Å), and their protonation and tautomeric states at pH 7.0 were generated using Epik^{30,31} (version 3.6, Schrödinger) and Spores.^{32,33}

Docking was performed using GOLD (version 5.3).^{34,35} Binding site residues were defined by specifying the crystal structure ligand coordinates bound to protein chains A and B and using the default cutoff radius of 6 Å, with the "detect cavity" option enabled. GOLD docking experiments were performed using the GoldScore scoring function. The search efficiency of the genetic algorithm was at 200% setting with the receptor kept rigid. For each compound, 50 complexes were generated and clustered based on their RMSD with the threshold set at 0.75 Å using the complete linkage method. Complexes were rescored using DrugScore (version 0.9)^{36–38} utilizing the DrugScore^{CSD} potential, and the best-ranked pose from each cluster was visually examined to select the final pose. The quality of pose prediction was assessed by calculating the heavy atom RMSD between the docked poses and the original PDB coordinates of strychnine (Figure S18, Supporting Information). The figures were prepared using PyMol.³⁹

■ ASSOCIATED CONTENT

Supporting Information

The Supporting Information is available free of charge on the ACS Publications website at DOI: 10.1021/acs.jnatprod.6b00479.

¹H and ¹³C NMR spectra of compounds **2**, **3**, **5**, and **6a–k**, traces of patch-clamp recordings and concentration response curves for strychnine and compounds **1–4**, **6a**, **6b**, **6h**, and **6i**, alignment of GlyR sequences from subtype α3 (PDB: 5CFB) and α1 (PDB: 3JAD), pose-retrieval docking data of the cocrystallized strychnine, overlay of the docked pose and PDB coordinates (5CFB) of strychnine, overlay of compounds **6i** and **6g** docked to the strychnine binding site of the α3 GlyR (PDF)

■ AUTHOR INFORMATION

Corresponding Author

*E-mail (D. Zlotos): darius.zlotos@guc.edu.edu.

ORCID

Hans-Georg Breiteringer: 0000-0003-0111-3528

Christoph Sottriffer: 0000-0003-4713-4068

Darius P. Zlotos: 0000-0002-1193-3119

Notes

The authors declare no competing financial interest.

■ ACKNOWLEDGMENTS

This work was partially funded by Bundesministerium für Bildung und Forschung (BMBF) and Deutscher Akademischer Austauschdienst (DAAD). A.A.J. thanks the Novo Nordisk Foundation for financial support.

■ REFERENCES

- (1) Lynch, J. W. *Physiol. Rev.* **2004**, *84*, 1051–1095.
- (2) Laube, B.; Maksay, G.; Schemm, R.; Betz, H. *Trends Pharmacol. Sci.* **2002**, *23*, 519–527.
- (3) Jensen, A. A.; Kristiansen, U. *Biochem. Pharmacol.* **2004**, *67*, 1789–1799.
- (4) Lynch, J.; Callister, R. *Curr. Opin. Invest. Drugs* **2006**, *7*, 48–53.
- (5) Breiteringer, H.-G. *eLS*; 2014, DOI: 10.1002/9780470015902.a0000236, pub2.
- (6) Breiteringer, H.-G.; Becker, C.-M. *Curr. Pharm. Design* **1998**, *4*, 315–334.
- (7) Bode, A.; Lynch, J. *Mol. Brain* **2014**, *7*, 2.
- (8) Schaefer, N.; Langlhofer, G.; Kluck, C. J.; Villmann, C. *Br. J. Pharmacol.* **2013**, *170*, 933–952.
- (9) Langosch, D.; Thomas, L.; Thomas, H. *Proc. Natl. Acad. Sci. U. S. A.* **1988**, *85*, 7394–7398.
- (10) Watanabe, E.; Akagi, H. *Neurosci. Res.* **1995**, *23*, 377–382.
- (11) Lynch, J. W. *Neuropharmacology* **2009**, *56*, 303–309.
- (12) Yu, R.; Hurdiss, E.; Greiner, T.; Lape, R.; Sivilotti, L.; Biggin, P. C. *Biochemistry* **2014**, *53*, 6041–6051.
- (13) Du, J.; Lü, W.; Wu, S.; Cheng, Y.; Gouaux, E. *Nature* **2015**, *526*, 224–229.
- (14) Huang, X.; Chen, H.; Michelsen, K.; Schneider, S.; Shaffer, P. L. *Nature* **2015**, *526*, 277–280.
- (15) Mackerer, C. R.; Kochman, R. L.; Shen, T. F.; Hershenson, F. M. *J. Pharmacol. Exp. Ther.* **1977**, *201*, 326–331.
- (16) Iskander, G. M.; Bohlin, L. *Acta Pharm. Suec.* **1978**, *15*, 431–438.
- (17) Jensen, A. A.; Gharagozloo, P.; Birdsall, N. J. M.; Zlotos, D. P. *Eur. J. Pharmacol.* **2006**, *539*, 27–33.
- (18) Mohsen, A. M. Y.; Heller, E.; Holzgrabe, U.; Zlotos, D. P. *Chem. Biodiversity* **2014**, *11*, 1256–1262.
- (19) Zlotos, D. P.; Buller, S.; Stiefl, N.; Baumann, K.; Mohr, K. J. *Med. Chem.* **2004**, *47*, 3561–3571.
- (20) Tang, P.; Furuya, T.; Ritter, T. *J. Am. Chem. Soc.* **2010**, *132*, 12150–12154.
- (21) Gharagozloo, P.; Lazareno, S.; Popham, A.; Birdsall, N. J. M. *J. Med. Chem.* **1999**, *42*, 438–445.

- (22) Rosenmund, P.; Schmitt, M.-P.; Franke, H. *Liebigs Ann. Chem.* **1980**, *6*, 895–907.
- (23) Jensen, A. A. *Eur. J. Pharmacol.* **2005**, *521*, 39–42.
- (24) Jensen, A. A.; Bergmann, M. L.; Sander, T.; Balle, T. *J. Biol. Chem.* **2010**, *285*, 10141–10153.
- (25) Hess, G. P. *Biochemistry* **1993**, *32*, 989–1000.
- (26) Breitingner, H. G.; Geetha, N.; Hess, G. P. *Biochemistry* **2001**, *40*, 8419–8429.
- (27) Raafat, K.; Breitingner, U.; Mahran, L.; Ayoub, N.; Breitingner, H.-G. *Toxicol. Sci.* **2010**, *118*, 171–182.
- (28) *Molecular Operating Environment (MOE)*, version 2013.08; Chemical Computing Group Inc: Montreal, QC, Canada, 2016.
- (29) Mostad, A. *Acta Chem. Scand.* **1985**, *B39* (9), 705–716.
- (30) Greenwood, J. R.; Calkins, D.; Sullivan, A. P.; Shelley, J. C. *J. Comput.-Aided Mol. Des.* **2010**, *24*, 591–604.
- (31) Shelley, J. C.; Cholleti, A.; Frye, L.; Greenwood, J. R.; Timlin, M. R.; Uchimaya, M. *J. Comput.-Aided Mol. Des.* **2007**, *21*, 681–691.
- (32) ten Brink, T.; Exner, T. E. *J. Chem. Inf. Model.* **2009**, *49*, 1535–1546.
- (33) ten Brink, T.; Exner, T. E. *J. Comput.-Aided Mol. Des.* **2010**, *24*, 935–942.
- (34) Jones, G.; Willett, P.; Glen, R. C. *J. Mol. Biol.* **1995**, *245*, 43–53.
- (35) Jones, G.; Willett, P.; Glen, R. C.; Leach, A. R.; Taylor, R. *J. Mol. Biol.* **1997**, *267*, 727–748.
- (36) Gohlke, H.; Hendlich, M.; Klebe, G. *J. Mol. Biol.* **2000**, *295*, 337–356.
- (37) Neudert, G.; Klebe, G. *J. Chem. Inf. Model.* **2011**, *51*, 2731–2745.
- (38) Velec, H. F.; Gohlke, H.; Klebe, G. *J. Med. Chem.* **2005**, *48*, 6296–303.
- (39) *PyMOL Molecular Graphics System*, Version 1.8; Schrödinger, LLC; 2015.